

Article

Analysis of Microwave Effects on the MnO₂-Catalyzed Toluene Oxidation Pathway

Fengming Yang¹, Yi Ye², Lili Ding^{3,4}, Huacheng Zhu⁵ , Jianhong Luo², Long Gao⁶, Yunfei Song^{3,4} and Shumeng Yin^{3,4,*}

- ¹ College of Computer Science and Cyber Security (Pilot Software College), Chengdu University of Technology, Chengdu 610059, China; fmyang2020@163.com
- ² Department of Chemical Engineering, Sichuan University, Chengdu 610065, China; 202323070028@stu.scu.edu.cn (Y.Y.); luojianhong@scu.edu.cn (J.L.)
- ³ SINOPEC Research Institute of Safety Engineering Co., Ltd., Qingdao 266100, China; dll3518@163.com (L.D.); 18321331680@163.com (Y.S.)
- ⁴ State Key Laboratory of Safety and Control for Chemicals, SINOPEC Research of Safety Engineering Co., Ltd., Qingdao 266071, China
- ⁵ College of Electronics and Information Engineering, Sichuan University, Chengdu 610065, China; hczyu@scu.edu.cn
- ⁶ Hefei Borei Electric Co., Ltd., Hefei 230031, China; gaolongdeyouxiang@126.com
- * Correspondence: yinshumeng@sinoproc.com

Abstract: Microwave radiation has become an effective catalytic combustion method, especially in the degradation of volatile organic compounds (VOCs) such as toluene using catalysts like MnO₂. In this study, a spine waveguide microwave reactor was designed to investigate the influence of different microwave processing conditions on the degradation of toluene catalyzed by MnO₂. An experimental system for microwave-assisted catalytic degradation of toluene was established to explore the relationship between microwave power, catalyst conductivity, and toluene degradation rate. The results showed that the efficiency of MnO₂ catalyzing toluene degradation had a nonlinear relationship with microwave power, first increasing to a peak and then decreasing. Additionally, the experiment found that the degradation rate of toluene was positively correlated with the conductivity of MnO₂. Subsequent characterization analyses using X-ray diffraction (XRD), X-ray photoelectron spectroscopy (XPS), and scanning electron microscopy (SEM) further verified the changes in the microstructure and properties of MnO₂ under microwave heating. The characterization results showed that with the increase in microwave power, the relative content of Mn³⁺ on the surface of MnO₂ increased, and the relative content of adsorbed oxygen also increased accordingly. At a microwave power of 100 W, the treated MnO₂ displayed the optimal ratio of manganese oxidation state and oxide, both close to 1:1, which was more conducive to the degradation of toluene. Based on these findings, this study hypothesized that the microwave-enhanced catalytic degradation of toluene by MnO₂ may be attributed to changes in the surface electron transfer kinetics of MnO₂, providing new insights into the field of microwave-enhanced catalysis.

Keywords: microwave heating; MnO₂; toluene; catalytic oxidation; transducer; conductivity



Citation: Yang, F.; Ye, Y.; Ding, L.; Zhu, H.; Luo, J.; Gao, L.; Song, Y.; Yin, S. Analysis of Microwave Effects on the MnO₂-Catalyzed Toluene Oxidation Pathway. *Processes* **2024**, *12*, 1074. <https://doi.org/10.3390/pr12061074>

Academic Editor: Maria Victoria Lopez-Ramon

Received: 5 April 2024

Revised: 13 May 2024

Accepted: 16 May 2024

Published: 24 May 2024



Copyright: © 2024 by the authors. Licensee MDPI, Basel, Switzerland. This article is an open access article distributed under the terms and conditions of the Creative Commons Attribution (CC BY) license (<https://creativecommons.org/licenses/by/4.0/>).

1. Introduction

Volatile organic compounds (VOCs) play a significant role in atmospheric pollution, contributing to the formation of ozone (O₃) and secondary aerosols, thereby exacerbating environmental issues such as haze and photochemical pollution [1–5]. These compounds, notorious for their unpleasant odors and health hazards including toxicity and carcinogenicity, pose serious threats to human health and ecological well-being [6–10]. With the proliferation of industrial activities, automobile emissions, and construction processes, VOC emissions have surged, intensifying the urgency to develop efficient, cost-effective, and energy-efficient methods for VOC degradation [11,12].

Currently, VOC treatment methods predominantly involve either recycling or destruction. Recycling techniques encompass physical adsorption, chemical absorption, and membrane separation [13–16]. While physical adsorption offers simplicity and cost-effectiveness, it lacks selectivity, necessitating further processing steps for effective separation of VOCs with differing values and environmental impacts. Conversely, chemical absorption and membrane separation methods exhibit high selectivity and purification efficiency but are hindered by elevated costs and technological complexity [17]. Destruction technologies, including photocatalytic degradation and catalytic combustion, have emerged as viable approaches for VOC remediation [18,19]. Although photocatalysis, particularly with TiO_2 as a catalyst, has demonstrated high degradation efficiency and environmental compatibility, its limitations, such as low energy utilization and sluggish reaction rates, remain a concern [20]. Catalytic combustion, on the other hand, offers a promising avenue for VOC treatment, with ongoing efforts focused on enhancing catalytic efficiency and addressing catalyst deactivation and durability issues through modification and optimization strategies [21].

Microwave irradiation, renowned for its efficient heating capabilities, presents a novel approach to catalytic VOC degradation. Differing from traditional heating methods, microwave heating ensures uniform heating throughout the catalyst, minimizing the risk of local temperature spikes that can lead to catalyst deactivation [22]. Additionally, microwave-assisted catalytic oxidation has shown greater efficiency compared to conventional thermal catalytic combustion, mainly due to enhanced mass transfer and reaction kinetics [23]. However, despite these advantages, the mechanism of microwave action remains unclear. Furthermore, there is a notable gap in research regarding the influence of microwave process parameters on the degradation pathways of VOCs. Recent studies have showcased the efficacy of microwave-enhanced catalysis using various catalysts, such as MnO_2 and Cu-Mn-Ce composites, in degrading VOCs like toluene, ethyl acetate, and acetone [24]. Mechanistic insights suggest that microwave irradiation induces changes in catalyst conductivity, facilitating electron transfer processes crucial for VOC oxidation [25].

MnO_2 is known for its strong microwave absorption and catalytic activity, making it a promising catalyst for microwave-assisted VOC degradation. MnO_2 's variable oxidation states facilitate electron transfer during the oxidation-reduction process, leading to the formation of more surface lattice defects and enhancing catalytic efficiency [26]. In this study, we aimed to track the variations in the conductivity of the MnO_2 catalyst under different microwave power levels. Our objective was to unveil the reaction pathway of toluene degradation catalyzed by MnO_2 under microwave irradiation and to elucidate the mechanism of microwave interaction with the catalyst. By elucidating the role of catalyst conductivity in VOC degradation, our research contributes to the development of more effective and energy-efficient VOC treatment methods.

2. Experiment and Material Characterization

2.1. Experiment of Conductivity Measurement and Microwave Enhancement

A comprehensive equipment setup was designed to monitor the temperature and conductivity of catalysts under microwave irradiation. A ridge waveguide was designed to provide uniform electric field to the heating area. The experimental setup included a microwave source capable of controlling power between 0 W and 200 W, a directional coupler with a microwave power meter, a microwave heating chamber, and a thermal imager. The catalyst was placed inside a quartz tube, with electrode plates tightly sealing both ends to ensure complete removal of air. The catalyst was only filled in the pores detectable by the thermal imaging instrument to ensure accurate temperature detection and a fixed amount of catalyst. The specific experimental system diagram is shown in Figure 1. Additionally, the experimental system for conductivity measurement during microwave heating is illustrated in Figure 2.

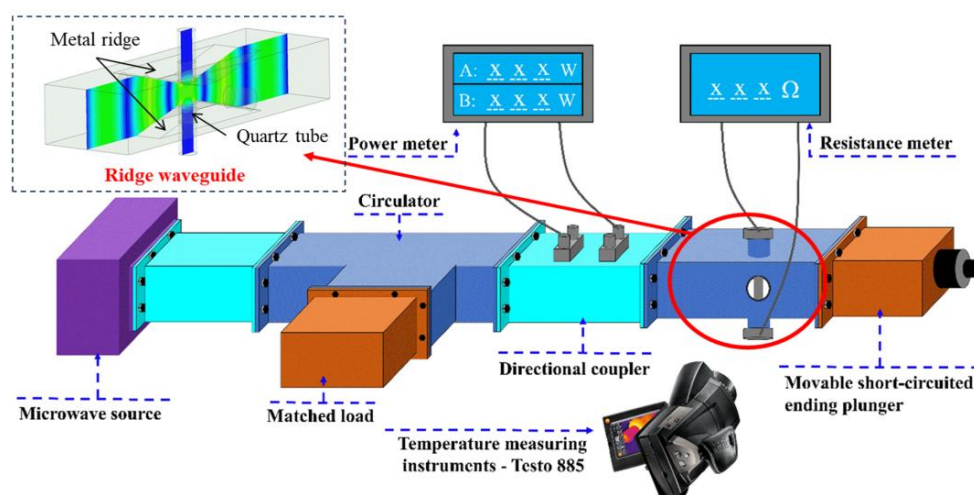


Figure 1. Experimental system diagram.

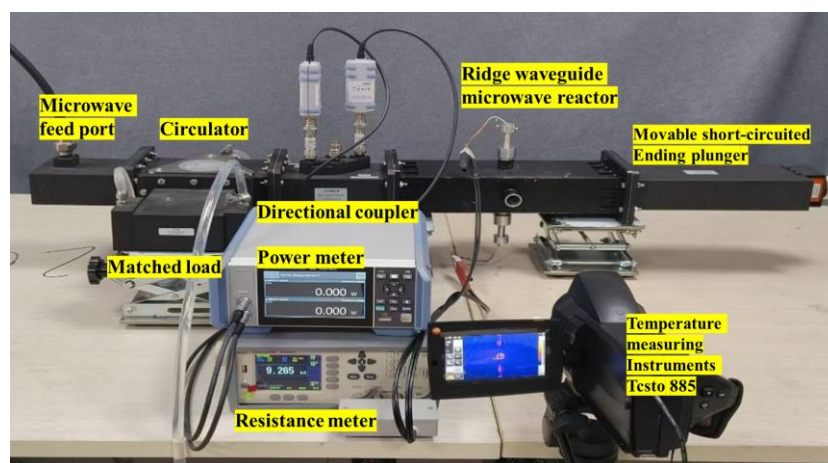


Figure 2. Experimental system.

The catalyst was prepared by mixing MnO_2 and Al_2O_3 at a ratio of 1:5. The mixture was then stirred at room temperature for 2 h to ensure uniform loading of MnO_2 onto the surface of the Al_2O_3 . The amount of catalyst used was 2 g per experiment. The MnO_2 catalyst used was of analytical grade and was purchased from Shanghai Macklin Biochemical Technology Co., Ltd., Shanghai, China.

The microwave power was set to 75 W, 100 W, and 125 W; the catalyst was heated with a microwave; the corresponding resistance at different temperatures (room temperature to 300 °C) was recorded by the thermal imager and ohmmeter; the microwave was turned off after microwave heating was completed; and the corresponding resistance at different temperatures was recorded when the catalyst was free cooling without the microwave. The catalyst conductivity was calculated using the following formula:

$$\sigma = \frac{L}{SR}, \quad (1)$$

where S is the area of the electrode piece, L is the relative distance between the two electrode pieces, and R is the resistance value of the measured material. In this experiment, $S = 1.54 \times 10^{-4} \text{ m}^2$, $L = 7.1 \times 10^{-2} \text{ m}$.

The device shown in Figure 2 was also used in the experiment of microwave-enhanced manganese dioxide catalytic oxidation of toluene. Air (O_2 21%, N_2 79%) was used as the background gas in the experiment; a quantitative amount of air and toluene were injected into a 20 L air bag to mix, and a concentration of about 700 ± 50 ppm of toluene was

obtained, which was uniformly fed into the microwave reactor using a constant flow pump, with a flow rate of 200 mL/min. After the system stabilized for 15 min, the inlet and outlet gases were measured. The concentration of the inlet and outlet gases was analyzed using gas chromatography–mass spectrometry (GC-MS) to obtain the toluene conversion rate. The conversion rate of toluene was calculated by the following formula:

$$\eta = \frac{C_{in} - C_{out}}{C_{in}} \times 100\%, \quad (2)$$

where C_{in} is the concentration of toluene in the incoming gas, and C_{out} is the concentration of toluene in the outgoing gas.

2.2. Catalyst Characterization Methods

The surface morphology characteristics of the catalyst samples were observed by scanning electron microscopy (SEM, ZEISS Sigma 300, Oberkochen, Germany). The X-ray diffraction pattern of the catalyst sample was obtained using an X-ray diffraction instrument (XRD, Rigaku Ultima IV, Tokyo, Japan). The test target was copper, with a scanning range of 5–90° and a step size of 0.02°. The elemental energy spectrum and valence distribution of the sample were measured using X-ray photoelectron spectroscopy (XPS, Thermo Scientific K-Alpha, Waltham, MA, USA).

3. Results and Discussion

3.1. The Relationship between Toluene Degradation Rate and Conductivity Changes under Microwave Irradiation

As shown in Figure 3a, the MnO₂ catalyst exhibited the best catalytic efficiency at a microwave power of 100 W. The results obtained were that the microwave had a strengthening effect on the catalytic oxidation of toluene by MnO₂, which presented a relationship similar to a “throwing line” rather than a simple positive correlation with microwave power. It is similar to the results reported in relevant reports [25]. Under the action of the microwave, MnO₂ exhibited good low-temperature catalytic activity for toluene. At 150 °C, the toluene degradation rates under 75 W, 100 W, and 125 W microwave power were able to reach 53.76%, 73.36%, and 59.01%, respectively. The effect of different microwave levels on the toluene degradation rate is more significant in the lower temperature region. As the temperature increases, the numerical performance of this effect gradually decreases because a microwave has both “thermal” and “non-thermal” effects on the catalyst itself [27]. In the low temperature range, the heating effect of a microwave on the catalyst has a smaller impact on the toluene degradation rate compared to “other effects”. As the temperature increases, the “thermal effect” dominates the degradation rate of toluene, while being accompanied by boundary effects, and the “non-thermal effect” of microwave is no longer significant. The T₉₀ under microwave irradiation of 100 W decreased by nearly 30 °C and 35 °C compared to 75 W and 125 W, respectively.

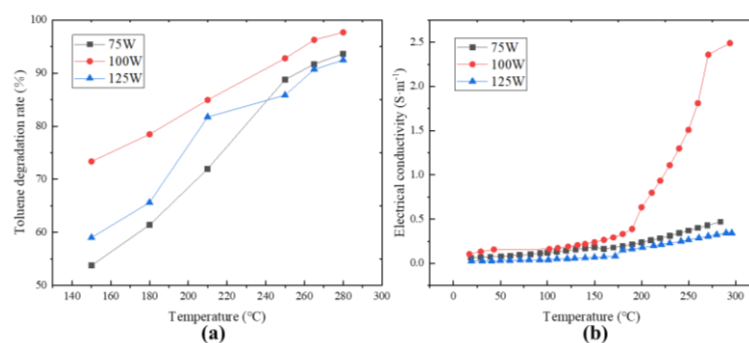


Figure 3. Temperature dependence of toluene degradation rate (a) and MnO₂ electrical conductivity (b) under different microwave power levels.

The catalytic degradation of toluene is essentially an electron transfer process. The existing microwave-enhanced catalytic mechanism has two main ways: one is that under the action of a microwave, there will be a photoelectric effect on the catalyst surface, and the electrons will be excited to escape from the catalyst surface and collide with gas molecules to form oxygen-free radicals, hydroxyl radicals, and other active components to degrade toluene. Another way occurs on the surface of the catalyst, where microwaves accelerate the adsorption of free oxygen molecules and the conversion to lattice oxygen, thereby accelerating the recovery of the catalyst and ultimately leading to an increase in toluene degradation rate [28]. Toluene and oxygen are adsorbed on the active site of the catalyst for a reaction. Thus, an electron transfer path can be constructed: toluene–MnO₂–oxygen, which means that the difficulty of electron transfer on the surface of the catalyst is likely to be an important indicator affecting the degradation rate of toluene. Figure 3b shows the variation of the conductivity of MnO₂ with increasing temperature under three different power levels. It can be seen that the conductivities of MnO₂ under the three power levels showed few changes and were close when the temperature was below 180 °C. The difference in conductivity gradually became apparent when the temperature was above 180 °C. The conductivity of MnO₂ at the power level of 100 W increased most significantly with the increase in temperature, and the entire conductivity changed in a “parabolic” shape, which is consistent with Figure 3a. There was almost no difference in conductivity among the three power levels between 150 °C and 180 °C, but the corresponding toluene degradation rate was far apart. It is speculated that the microwave may have other effects besides changing the catalyst conductivity to affect its toluene degradation rate. In addition, it was observed that the conductivity under the action of 75 W was always higher than 125 W, but the toluene degradation rate under the action of 75 W was only higher than 125 W when the temperature reached 250 °C. Fresh MnO₂ heated up slowly at first, but the heating rate increased after a certain period of heating, which is inconsistent with heat transfer theory. These also indicate that microwave-enhanced MnO₂ catalytic oxidation of toluene may not only be achieved by changing the conductivity [29].

Figure 4 shows the comparison of conductivity changes between microwave heating and free cooling, as well as the comparison of conductivity changes after microwave treatment with different power levels. It can be seen that the conductivity of free cooling MnO₂ after microwave treatment was higher than that during microwave heating, and no other gas entered the catalyst phase in the experiment, which can exclude the change of the catalyst due to the reaction of contacting toluene. It is worth noting that Figure 3b shows fresh MnO₂ that had not been microwave treated. Its initial conductivity at room temperature was consistent, but after microwave treatment, it showed differences at room temperature. Overall, the conductivity showed a pattern of 100 W > 75 W > 125 W, which is sufficient to indicate that microwave action changed some properties of MnO₂.

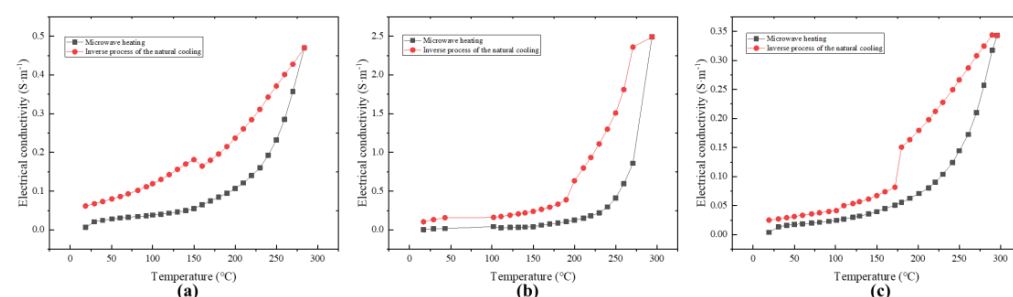


Figure 4. Comparison of electrical conductivity changes between microwave power heating and free cooling: (a) 75 W, (b) 100 W, (c) 125 W.

From the above experimental results, it can be preliminarily determined that the efficiency of MnO₂ catalytic degradation of toluene is related to the changes in the conductivity of the catalyst itself. Microwave can further enhance the conductivity of MnO₂

and strengthen the toluene degradation process through the “non thermal effect”. The microstructure of MnO_2 after microwave treatment underwent certain changes, which may also be the key to the microwave strengthening process.

The catalytic oxidation of toluene is essentially an electron transfer process, so a reaction process is proposed: toluene loses electrons after being adsorbed on the active site of the MnO_2 surface, electrons are transmitted to the surface-adsorbed oxygen through the catalyst itself, and the oxidized toluene forms degradation products with lattice oxygen. This process can be seen as a microscopic closed circuit, so the difficulty of electron transfer in MnO_2 itself and the proportion of different valence states of related elements may be the key to the catalytic efficiency. The experiment shows that MnO_2 exhibited different conductivity changes under the action of different microwave power levels. The conductivity change of MnO_2 is similar to a “parabolic” form, which is also consistent with the toluene degradation rate measured under the same conditions. This result proves that microwaves can enhance the toluene degradation process by changing the conductivity of MnO_2 , and this also proves the accuracy and reliability of the reaction process proposed in the experiment. In addition, it was observed that the conductivity of MnO_2 after microwave treatment cannot be restored to its initial state and is always higher than the conductivity during microwave heating. It is speculated that the change in conductivity measured macroscopically is actually a change in the microstructure of MnO_2 under the action of a microwave.

3.2. Catalyst Characterization

3.2.1. XRD Characterization

Figure 5 shows the XRD pattern of the MnO_2 catalyst after microwave treatment with different power levels. It was observed that the crystallinity of the MnO_2 catalyst was relatively low, with the peaks of 2θ at 37.32° (211), 42.66° (301), 56.66° (600), and 65.46° (002) retrieved as MnO_2 crystalline phases (PDF # 44-0141). The MnO_2 after 100 W microwave treatment exhibited stronger diffraction peaks on the (211) and (600) crystal planes. This may have been caused by the high lattice defects and low crystallinity of the MnO_2 catalyst itself in that all diffraction peaks deviated towards the direction of larger 2θ angles. For the MnO_2 treated after a 125 W microwave, Mn_2O_3 of the type of bixbyite-C were also able to be retrieved, and the diffraction peaks were particularly consistent with the standard card, indicating that MnO_2 underwent changes in valence and structure under the action of the microwave. The peak intensity order of the (222) crystal plane corresponding to standard card PDF # 41-1442 in the four spectral lines was MnO_2 —125 W > MnO_2 —100 W > MnO_2 —75 W > MnO_2 —fresh. What is even more noteworthy is that MnO_2 will gradually convert to Mn_2O_3 under the action of a microwave, and the $\text{Mn}^{3+}/\text{Mn}^{4+}$ of MnO_2 itself is related to the catalytic efficiency [30].

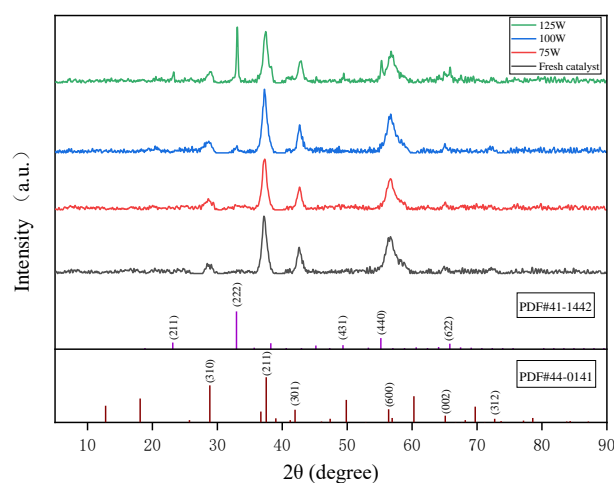


Figure 5. XRD patterns of MnO_2 after different microwave treatments.

3.2.2. XPS Characterization

The surface chemical composition and valence states of MnO₂ treated with different microwave powers were studied through XPS characterization. The XPS spectra of Mn 2p and O 1s of treated MnO₂ are shown in Figure 6. The asymmetric peak at 641.7 eV in Figure 6a can be attributed to the Mn 2p^{3/2} peak, which can be divided into the Mn³⁺ peak at 641.5 eV and the Mn⁴⁺ peak at 642.4 eV. The relative content of two different valence states of Mn elements was able to be obtained by calculating the peak area. As the microwave power increased, the content of Mn³⁺ increased, which is consistent with the XRD results in Figure 5 and also proves that the structure and even chemical valence state of MnO₂ after microwave treatment changed [30]. The catalytic oxidation of toluene by MnO₂ is essentially an electron transfer process. Toluene combines with the lattice oxygen in the catalyst to generate CO₂ (an intermediate will be generated when the reaction is incomplete) with the loss of electron. The Mn⁴⁺ in the catalyst changes to Mn³⁺ by obtaining electrons, and then the Mn³⁺ transfers electrons to the surface-adsorbed oxygen, reducing and converting O_{ads} into O_{latt}, as shown in Figure 6c. This electron transfer pathway clearly has a rate control step and can exhibit the best catalytic efficiency when Mn³⁺/Mn⁴⁺ and O_{ads}/O_{latt} are close to 1 [31–33].

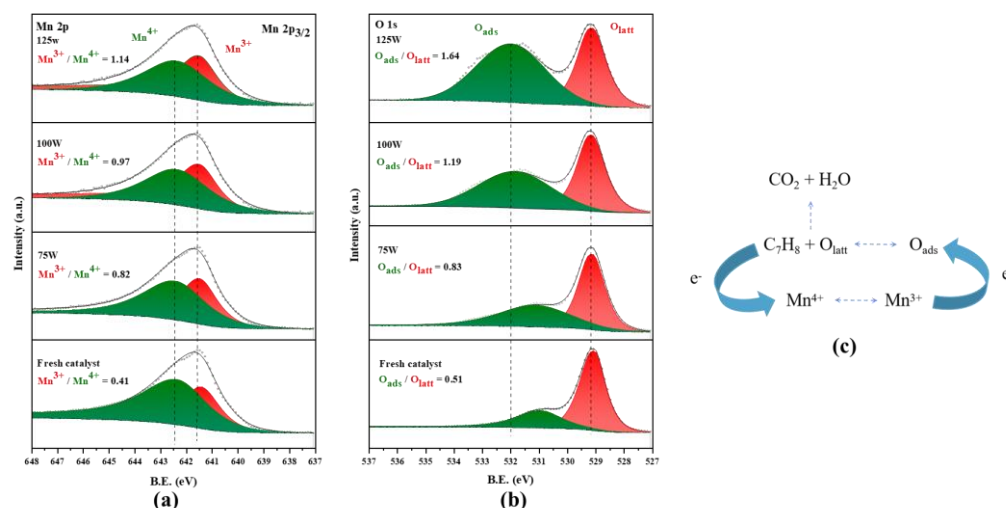


Figure 6. XPS spectra of various elements after microwave treatment at different powers: (a) Mn 2p; (b) O 1s. Electron transfer process of MnO₂-catalyzed oxidation of toluene (c).

The oxygen species peak shown in Figure 6b was able to be divided into a O_{latt} peak at 529.10 eV and a O_{ads} peak at 531–532 eV. The relative content of O_{ads} also increased with the increase in microwave power, which was consistent with the growth pattern of Mn³⁺. The conversion of lattice oxygen to adsorbed oxygen will cause lattice loss and charge imbalance, with some Mn⁴⁺ being converted into Mn³⁺. It was observed that under the action of the microwave, the best catalytic efficiency was not the 125 W treated MnO₂ with the highest relative content of O_{ads}. According to the usual theory, the increase in O_{ads} is accompanied by more oxygen vacancies and more active site of the catalyst, which is conducive to the improvement of catalytic efficiency. This may be due to the close content of O_{ads} and O_{latt} in MnO₂ treated with 100 W, and the ratio of O_{ads} and Mn³⁺ being the closest to charge transfer [33]. The combination of these factors ultimately leads to the best catalytic efficiency of MnO₂ under 100 W microwave irradiation. In addition, it can also be observed from Figure 6b that the peak of O_{ads} shifted to a higher binding energy with the increase in microwave power, which indicates that the adsorbed oxygen formed was more stable and more oxidizing.

3.2.3. SEM Characterization

Figure 7 shows the SEM images of MnO_2 after four different power microwave treatments. It can be seen that the fresh catalyst shown in Figure 7a,b without microwave treatment was mainly composed of nanowires, nanoparticles, and nanosheets. The nanowires were relatively short, ranging in length from 100 nm to 300 nm, with nanoparticles and nanosheets attached to the nanowires. Compared with fresh catalysts, the MnO_2 shown in Figure 7c,d treated with 75 W microwave power had significantly shorter and thicker nanowires, while the MnO_2 shown in Figure 7e,f treated with 100 W microwave power had longer and more clearly formed nanowires compared to the first two, and the nanoparticles were more uniformly attached to the nanowires. The nanowires of the MnO_2 shown in Figure 7g,h treated with 125 W microwave power become shorter and fewer than that of fresh MnO_2 , with the proportion of nanoparticles increasing overall.

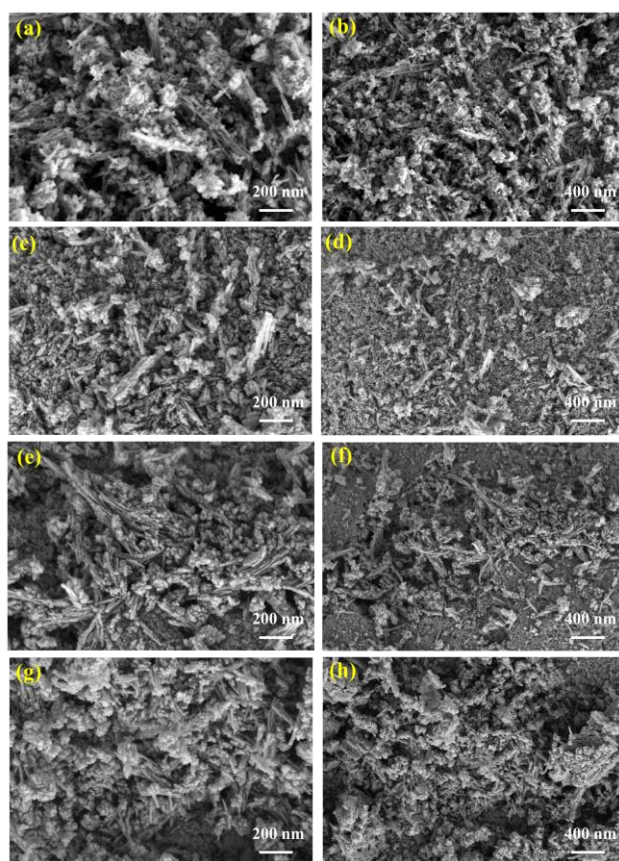


Figure 7. SEM images of MnO_2 after microwave treatment under different microwave power levels. (a,b) Fresh; (c,d) after 75 W microwave treatment; (e,f) after 100 W microwave treatment; (g,h) after 125 W microwave treatment.

There were significant microscopic differences in the microstructure of MnO_2 of four different states, indicating that within the same temperature growth range, different powers of microwaves also had corresponding effects on the microstructure of MnO_2 . This may also be one of the reasons for the change in conductivity of the catalyst under and after microwave influence [34–36].

The characterization results of XRD, XPS, and SEM show that the microwave did have an impact on the structure and surface elemental valence of MnO_2 . The XRD results show that with the increase in microwave power, a portion of MnO_2 gradually transformed into Mn_2O_3 , and the XPS results clearly prove this: as the microwave power increased, the relative content of Mn^{3+} on the surface of MnO_2 gradually increased, and the corresponding relative content of Oads also gradually increased. At the microwave power of 100 W, the

treated MnO₂ exhibited the best Mn element valence state ratio and oxygen species ratio, both of which were closer to 1:1. This also indicates that the equilibrium valence state ratio and oxygen species ratio were more conducive to the degradation of toluene.

4. Conclusions

Microwave irradiation enhances the catalytic oxidation of toluene by MnO₂ without directly affecting toluene degradation. To investigate this enhancement mechanism, we designed a microwave heating device to measure the conductivity change of MnO₂ under different microwave power levels. Concurrently, we measured the change in toluene degradation rate. Our results reveal that the catalytic oxidation of toluene on the MnO₂ surface involves an electron transfer process, where toluene loses electrons, and the oxidized toluene forms degradation products with lattice oxygen. Microwave irradiation enhances this process by changing the conductivity of MnO₂, as evidenced by “parabolic” conductivity changes that correlate with toluene degradation rates. Furthermore, microwave treatment altered the microstructure of MnO₂, as evidenced by XRD, XPS, and SEM analyses, resulting in an increase in Mn³⁺ content and oxygen adsorption. At 100 W microwave power, MnO₂ exhibited the optimal Mn oxidation state and oxygen species ratio, facilitating toluene degradation. Our experiments have demonstrated the proposed “micro closed circuit” reaction process. The degradation rate of toluene is positively correlated with the conductivity change of MnO₂ under microwave irradiation. Under 100 W irradiation, the T90 decreased by nearly 30 °C and 35 °C compared to 75 W and 100 W, respectively. Microwave irradiation can also alter the structure and valence distribution of MnO₂ itself. The characterization results obtained validate the mechanism of microwave-enhanced MnO₂ catalytic oxidation of toluene. These results have significant implications for the development of more efficient and energy-effective VOC treatment methods. This research holds promise for industrial applications, particularly in VOC cleanup processes.

Author Contributions: F.Y.: writing—original draft, writing—review and editing; Y.Y.: investigation; L.D.: data curation; H.Z.: conceptualization, validation; J.L.: formal analysis; L.G.: data curation; Y.S.: visualization. S.Y.: writing—original draft, resources. All authors have read and agreed to the published version of the manuscript.

Funding: This research was by the National Natural Science Foundation of China under grant no. 62001130, the National Key Research and Development Plan under grant no. 2023YFB4603501, and Hefei City unveils major projects under grant no. 2022-SZD-004.

Data Availability Statement: The data presented in this study are available on request from the corresponding author.

Conflicts of Interest: Authors Lili Ding, Yunfei Song and Shumeng Yin were employed by the company SINOPEC Research Institute of Safety Engineering Co., Ltd. and SINOPEC Research of Safety Engineering Co., Ltd. Author Long Gao was employed by the company Hefei Borei Electric Co., Ltd. The remaining authors declare that the research was conducted in the absence of any commercial or financial relationships that could be construed as a potential conflict of interest. The SINOPEC Research Institute of Safety Engineering Co., Ltd., SINOPEC Research of Safety Engineering Co., Ltd. and Hefei Borei Electric Co., Ltd. had no role in the design of the study; in the collection, analyses, or interpretation of data; in the writing of the manuscript, or in the decision to publish the results.

References

1. Wu, J.; Zhu, X.; Cai, Y.; Tu, X.; Gao, X. Coupling nonthermal plasma with V₂O₅/TiO₂ nanofiber catalysts for enhanced oxidation of ethyl acetate. *Ind. Eng. Chem. Res.* **2019**, *58*, 2–10. [[CrossRef](#)]
2. Li, Z.; Liu, J.; Gao, B.; Bo, L. Cu-Mn-CeOx loaded ceramic catalyst for non-thermal sterilization and microwave thermal catalysis of VOCs degradation. *Chem. Eng. J.* **2022**, *442*, 136288. [[CrossRef](#)]
3. Saoud, W.A.; Kane, A.; Le Cann, P.; Gerard, A.; Lamaa, L.; Peruchon, L.; Brochier, C.; Bouzaza, A.; Wolbert, D.; Assadi, A.A. Innovative photocatalytic reactor for the degradation of VOCs and microorganism under simulated indoor air conditions: Cu-Ag/TiO₂-based optical fibers at a pilot scale. *Chem. Eng. J.* **2021**, *411*, 128622. [[CrossRef](#)]

4. Zhang, X.; Wang, J. Dose-response relation deduced for coronaviruses from coronavirus disease 2019, severe acute respiratory syndrome, and middle east respiratory syndrome: Meta-analysis results and its application for infection risk assessment of aerosol transmission. *Clin. Infect. Dis.* **2021**, *73*, e241–e245. [[CrossRef](#)]
5. Kurniawan, T.A.; Haider, A.; Ahmad, H.M.; Mohyuddin, A.; Aslam, H.M.U.; Nadeem, S.; Javed, M.; Othman, M.H.D.; Goh, H.H.; Chew, K.W. Source, occurrence, distribution, fate, and implications of microplastic pollutants in freshwater on environment: A critical review and way forward. *Chemosphere* **2023**, *325*, 138367. [[CrossRef](#)] [[PubMed](#)]
6. Kuang, H.; Li, Z.; Lv, X.; Wu, P.; Tan, J.; Wu, Q.; Li, Y.; Jiang, W.; Pang, Q.; Wang, Y.; et al. Exposure to volatile organic compounds may be associated with oxidative DNA damage-mediated childhood asthma. *Ecotoxicol. Environ. Saf.* **2021**, *210*, 111864. [[CrossRef](#)] [[PubMed](#)]
7. Bari, M.A.; Kindzierski, W.B. Ambient volatile organic compounds (VOCs) in communities of the Athabasca oil sands region: Sources and screening health risk assessment. *Environ. Pollut.* **2018**, *235*, 602–614. [[CrossRef](#)] [[PubMed](#)]
8. Kuranchie, F.A.; Angnunavuri, P.N.; Attiogbe, F.; Nerquaye-Tetteh, E.N. Occupational exposure of benzene, toluene, ethylbenzene and xylene (BTEX) to pump attendants in Ghana: Implications for policy guidance. *Cogent. Environ. Sci.* **2019**, *5*, 1603418. [[CrossRef](#)]
9. Brummer, V.; Teng, S.Y.; Jecha, D.; Skryja, P.; Vavrcikova, V.; Stehlik, P. Contribution to cleaner production from the point of view of VOC emissions abatement: A review. *J. Clean. Prod.* **2022**, *361*, 132112. [[CrossRef](#)]
10. Guo, Y.; Wen, M.; Li, G.; An, T. Recent advances in VOC elimination by catalytic oxidation technology onto various nanoparticles catalysts: A critical review. *Appl. Catal. B Environ.* **2021**, *281*, 119447. [[CrossRef](#)]
11. Wang, Y.; Ding, L.; Shi, Q.; Liu, S.; Qian, L.; Yu, Z.; Wang, H.; Lei, J.; Gao, Z.; Long, H.; et al. Volatile organic compounds (VOC) emissions control in iron ore sintering process: Recent progress and future development. *Chem. Eng. J.* **2022**, *448*, 137601. [[CrossRef](#)]
12. Zhao, Z.; Ma, S.; Gao, B.; Bi, F.; Qiao, R.; Yang, Y.; Wu, M.; Zhang, X. A systematic review of intermediates and their characterization methods in VOCs degradation by different catalytic technologies. *Sep. Purif. Technol.* **2023**, *314*, 123510. [[CrossRef](#)]
13. Zhao, Q.; Zhao, Z.; Rao, R.; Yang, Y.; Ling, S.; Bi, F.; Shi, X.; Xu, J.; Lu, G.; Zhang, X. Universitetet i Oslo-67 (UiO-67)/graphite oxide composites with high capacities of toluene: Synthesis strategy and adsorption mechanism insight. *J. Colloid Interface Sci.* **2022**, *627*, 385–397. [[CrossRef](#)] [[PubMed](#)]
14. Zhao, Q.; Du, Q.; Yang, Y.; Zhao, Z.; Cheng, J.; Bi, F.; Shi, X.; Xu, J.; Zhang, X. Effects of regulator ratio and guest molecule diffusion on VOCs adsorption by defective UiO-67: Experimental and theoretical insights. *Chem. Eng. J.* **2022**, *433*, 134510. [[CrossRef](#)]
15. Li, X.; Zhang, L.; Yang, Z.; Wang, P.; Yan, Y.; Ran, J. Adsorption materials for volatile organic compounds (VOCs) and the key factors for VOCs adsorption process: A review. *Sep. Purif. Technol.* **2020**, *235*, 116213. [[CrossRef](#)]
16. Liang, H.; Wu, G.; Zhang, H.; Liu, Q.; Yang, Q.; Xiong, S.; Yue, Y.; Yuan, P. Controllable synthesis of N-doped hollow mesoporous carbon with tunable structures for enhanced toluene adsorption. *Sep. Purif. Technol.* **2022**, *283*, 120171. [[CrossRef](#)]
17. Wang, Y.; Su, Y.; Yang, L.; Su, M.; Niu, Y.; Liu, Y.; Sun, H.; Zhu, Z.; Liang, W.; Li, A. Highly efficient removal of PM and VOCs from air by a self-supporting bifunctional conjugated microporous polymers membrane. *J. Membr. Sci.* **2022**, *659*, 120728. [[CrossRef](#)]
18. Rao, R.; Ma, S.; Gao, B.; Bi, F.; Chen, Y.; Yang, Y.; Liu, N.; Wu, M.; Zhang, X. Recent advances of metal-organic framework-based and derivative materials in the heterogeneous catalytic removal of volatile organic compounds. *J. Colloid Interface Sci.* **2023**, *636*, 55–72. [[CrossRef](#)]
19. Almaie, S.; Vatanpour, V.; Rasoulifard, M.H.; Koyuncu, I. Volatile organic compounds (VOCs) removal by photocatalysts: A review. *Chemosphere* **2022**, *306*, 135655. [[CrossRef](#)]
20. Haidry, A.A.; Yucheng, W.; Fatima, Q.; Raza, A.; Zhong, L.; Chen, H.; Mandebvu, C.R.; Ghani, F. Synthesis and characterization of TiO₂ nanomaterials for sensing environmental volatile compounds (VOCs): A review. *TrAC Trends Anal. Chem.* **2023**, *170*, 117454. [[CrossRef](#)]
21. Gao, W.; Tang, X.; Yi, H.; Jiang, S.; Yu, Q.; Xie, X.; Zhuang, R. Mesoporous molecular sieve-based materials for catalytic oxidation of VOC: A review. *J. Environ. Sci.* **2023**, *125*, 112–134. [[CrossRef](#)] [[PubMed](#)]
22. Wang, Y.; Chen, W.; Zhou, Y.; Zhong, Y.; Zhong, N.; Jia, S.; Huang, K. Investigation of microwave enhanced catalytic degradation of VOCs with a novel double ridge field compressed cavity. *Chem. Eng. J.* **2022**, *442*, 136181. [[CrossRef](#)]
23. Yi, H.; Song, L.; Tang, X.; Zhao, S.; Yang, Z.; Xie, X.; Ma, C.; Zhang, Y.; Zhang, X. Effect of microwave absorption properties and morphology of manganese dioxide on catalytic oxidation of toluene under microwave irradiation. *Ceram. Int.* **2020**, *46*, 3166–3176. [[CrossRef](#)]
24. Wang, Y.; Chen, W.; Zhong, Y.; Zhong, N.; Huang, K. A study of microwave-enhanced catalytic degradation of benzene using Co-Mn metal oxides combined with numerical simulation. *Chem. Eng. Process.-Process Intensif.* **2023**, *189*, 109403. [[CrossRef](#)]
25. Feng, S.; Liu, J.; Gao, B. Synergistic mechanism of Cu-Mn-Ce oxides in mesoporous ceramic base catalyst for VOCs microwave catalytic combustion. *Chem. Eng. J.* **2022**, *429*, 132302. [[CrossRef](#)]
26. Zhang, X.; Hayward, D.O.; Mingos, D.M.P. Apparent equilibrium shifts and hot-spot formation for catalytic reactions induced by microwave dielectric heating. *Chem. Commun.* **1999**, 975–976. [[CrossRef](#)]
27. Zhou, Y.H.; Lei, X.X.; Zhou, J.Y.; Yan, D.L.; Deng, B.; Liu, Y.D.; Xu, W.L. Recent Advances in the Regulation of Oxygen Vacancies in MnO₂ Nanocatalysts. *Catal. Surv. Asia* **2023**, *27*, 319–331. [[CrossRef](#)]

28. Yang, Z.; Yi, H.; Tang, X.; Zhao, S.; Huang, Y.; Xie, X.; Song, L.; Zhang, Y. Study of reaction mechanism based on further promotion of low temperature degradation of toluene using nano-CeO₂/Co₃O₄ under microwave radiation for cleaner production in spraying processing. *J. Hazard. Mater.* **2019**, *373*, 321–334. [[CrossRef](#)]
29. Ding, S.; Zhu, C.; Hojo, H.; Einaga, H. Enhanced catalytic performance of spinel-type Cu-Mn oxides for benzene oxidation under microwave irradiation. *J. Hazard. Mater.* **2022**, *424*, 127523. [[CrossRef](#)]
30. Zeng, J.; Xie, H.; Zhang, H.; Huang, M.; Liu, X.; Zhou, G.; Jiang, Y. Insight into the effects of oxygen vacancy on the toluene oxidation over α -MnO₂ catalyst. *Chemosphere* **2022**, *291*, 132890. [[CrossRef](#)]
31. Luo, Y.; Zheng, Y.; Zuo, J.; Feng, X.; Wang, X.; Zhang, T.; Zhang, K.; Jiang, L. Insights into the high performance of Mn-Co oxides derived from metal-organic frameworks for total toluene oxidation. *J. Hazard. Mater.* **2018**, *349*, 119–127. [[CrossRef](#)] [[PubMed](#)]
32. Wang, P.; Zhao, J.; Zhao, Q.; Ma, X.; Du, X.; Hao, X.; Tang, B.; Abudula, A.; Guan, G. Microwave-assisted synthesis of manganese oxide catalysts for total toluene oxidation. *J. Colloid Interface Sci.* **2022**, *607*, 100–110. [[CrossRef](#)]
33. Yang, W.; Su, Z.; Xu, Z.; Yang, W.; Peng, Y.; Li, J. Comparative study of α -, β -, γ - and δ -MnO₂ on toluene oxidation: Oxygen vacancies and reaction intermediates. *Appl. Catal. B Environ.* **2020**, *260*, 118150. [[CrossRef](#)]
34. Song, L.; Duan, Y.; Liu, J.; Pang, H. Transformation between nanosheets and nanowires structure in MnO₂ upon providing Co²⁺ ions and applications for microwave absorption. *Nano Res.* **2020**, *13*, 95–104. [[CrossRef](#)]
35. Zhu, T.; Wang, R.; Yang, J.; Wang, C.; Wang, W.; Yang, W. Novel hollow urchin-like α/γ -MnO₂ boost microwave absorption. *J. Mater. Sci. Mater. Electron.* **2023**, *34*, 2149. [[CrossRef](#)]
36. Baral, A.; Satish, L.; Zhang, G.; Ju, S.; Ghosh, M.K. A review of recent progress on nano MnO₂: Synthesis, surface modification and applications. *J. Inorg. Organomet. Polym. Mater.* **2021**, *31*, 899–922. [[CrossRef](#)]

Disclaimer/Publisher's Note: The statements, opinions and data contained in all publications are solely those of the individual author(s) and contributor(s) and not of MDPI and/or the editor(s). MDPI and/or the editor(s) disclaim responsibility for any injury to people or property resulting from any ideas, methods, instructions or products referred to in the content.